Eur. Phys. J. B **19**, 171–176 (2001)

THE EUROPEAN PHYSICAL JOURNAL B

EDP Sciences

Ferroelastic domain structure of $(CH_3)_4N$ $CdCl_3$ (TMCC) crystal

T. Breczewski[1,a], I. Peral[2,b], and G. Madariaga[2]

[1] Departamento de Física Aplicada II, Facultad de Ciencias, Universidad del País Vasco, Apdo. 644, 48080 Bilbao, Spain
[2] Departamento de Física de la Materia Condensada, Facultad de Ciencias, Universidad del País Vasco, Apdo. 644, 48080 Bilbao, Spain

Received 21 July 2000

Abstract. The ferroelastic domain structure and the phase boundaries of TMCC have been studied in the temperature range 114–90 K by direct observation under polarised light. By applying an external, compressive and unidirectional mechanical stress the ferroelastic character of the domain structure has been confirmed. The orientation of the domain walls and phase boundaries are analysed. To characterise quantitatively the observed domain wall distribution the classical symmetry approach, based on the criterion of spontaneous strain compatibility, has to be extended to allow small rotations of the domain walls with respect to their ideal orientation. The observed switching process among the different domains can be understood as a mechanism that minimises the elastic energy.

PACS. 68.35.Rh Phase transitions and critical phenomena – 75.60.Ch Domain walls and domain structure

1 Introduction

Most of the members of the family of compounds of the type $[(CH_3)_4N]$ MX_3 (M: divalent metal = Cd, Mn, Ni, Cu, V, Pb; X: halogen = Cl, Br, I) share at room temperature a common hexagonal structure [1]. It can be described by linear and parallel chains $[MX_6]_\infty$ of stacked octahedra sharing opposite faces and tetrahedral organic $(CH_3)_4N$ groups located between the chains in planes perpendicular to them. The relative orientation of the symmetry elements of the organic groups with respect to the point group of the sites they occupy provokes a statistical disorder of $(CH_3)_4N$ among several orientations related by those crystallographic elements not belonging to the intersection of both point groups.

All of these compounds undergo several structural phase transitions as the temperature decreases. Some of them are expected to be ferroelastic. This is the case of $[(CH_3)_4N]CdCl_3$, $[(CH_3)_4N]MnCl_3$, $[(CH_3)_4N]MnBr_3$ and $[(CH_3)_4N]NiBr_3$.

Considerable effort has been made, in particular with $[(CH_3)_4N]MnCl_3$ and $[(CH_3)_4N]CdCl_3$, to explain the transition mechanism which is commonly associated with ordering processes involving $[(CH_3)_4N]$ groups, without important modifications in the inorganic chains [2].

In the case of $[(CH_3)_4N]CdCl_3$, two successive structural first order phase transitions have been observed at 118 K and 104 K, respectively [3–6]. The former one connects the hexagonal (space group $P6_3/m$, $Z = 2$) phase (I) with a monoclinic phase (II) with space group $P2_1/m$ and $Z = 2$. The latter leads to another monoclinic phase (III) with space group $P2_1/b$ and $Z = 12$ [2,7].

A structural solution of the low temperature phases could confirm the proposed phase transition schemes. However, this is not a trivial task since the appearance of ferroelastic domains prevents even a precise determination of the low temperature space groups and only the low temperature structures of $[(CH_3)_4N]MnCl_3$ and $[(CH_3)_4N]CdBr_3$ are known. For this latter (particularly favourable) compound, the order-disorder character of the phase transition has been established [8].

As was discussed by Peral *et al.* [7], the monoclinic low temperature phases of the ferroelastic compounds of this family contain a number of ferroelastic domains that do not fit with the quotient between the paraelastic and ferroelastic point group orders.

However, the structure of the orientation domains observed in X-ray diffraction diagrams [7] and NMR studies [3] of $[(CH_3)_4N]CdCl_3$, the diffraction diagrams and the antiferromagnetic resonance measurements in $[(CH_3)_4N]MnBr_3$ [9,10] and the neutron diffraction patterns of $[(CH_3)_4N]NiBr_3$ [11] can be explained using the approach proposed by Shuvalov and Dudnik [12,13].

The most important contributions of the present work are firstly the confirmation of the ferroelastic character of the orientation domains in $[(CH_3)_4N]CdCl_3$ and secondly the observation of the domain walls and phase

[a] e-mail: wdpbrxxt@lg.ehu.es
[b] e-mail: wmbpeali@lg.ehu.es

boundaries predicted by the Shuvalov and Dudnik approach which is based on an earlier mathematical treatment of the orientation of interphase boundaries in martensites (see [12,13,18] and references therein).

2 Experimental procedure

Crystals of $[(CH_3)_4N]CdCl_3$ (TMCC) were grown from a saturated stoichiometric, acid aqueous solution (pH < 3) of $[(CH_3)_4N]Cl$ and $CdCl_2$ compounds by the dynamic method. The obtained single crystals were of good optical quality, colourless, transparent and in the shape of a prism with hexagonal base and an edge length between 5 and 20 mm.

Samples to be studied were cut out as rectangular parallelepipeds $4 \times 5 \times 1$ mm^3 in size with edges parallel to each of the crystallographic axes of the hexagonal phase with polished surfaces perpendicular to the c-axis.

Samples were heated and cooled using a heating stage THMS 600 (Linkam) which was adapted to apply uniaxial strains. Temperature was controlled within ± 0.1 °C. Optical observations were performed along the c-axis using a polarizing microscope (Axioplan 2 - Carl Zeiss Jena) equipped with a digital camera (Polaroid DMC Digital Microscope Camera) of high resolution (1200×1600 pixels). The angles between the domain walls and the crystallographic axes were measured using the KS100 Imaging System (Carl Zeiss Jena) computer program. All angle measurements and calculations are referred to a common Cartesian frame, fixed in the paraelectric phase. The Cartesian z-axis has been chosen along the sixfold axis. The y-axis is parallel to the crystallographic b-axis which is common to the three studied phases. The optical observations were continuous in a temperature range (293–90 K) that includes two phase transitions relating the phases I–II and II–III respectively.

3 Experimental results

Figures 1 and 2 show a typical distribution of the phase boundary[1], between the hexagonal phase I and the monoclinic phase II, during cooling (Fig. 1) and heating (Fig. 2) respectively. During the cooling process characteristic strips, making angles of 111.6° with the x-axis of the orthogonal system, appear. Inside them are located domain walls tilted about 62° and 162° with respect to the x-axis. The curvilinear shape of the walls prevent an accurate measurement of such angles. In some places the strips are broken and there appear phase boundaries whose inclination respect the x-axis is about 143.5°. During heating (Fig. 2) the phase boundary has almost the shape of a straight line and makes an angle of 50.5° with the x-axis.

In the ferroelastic phase (Fig. 3) the size of the domains is very small compared with those occurring commonly in

[1] Strictly speaking we are referring to the projection of phase boundaries and domain walls as seen through the microscope.

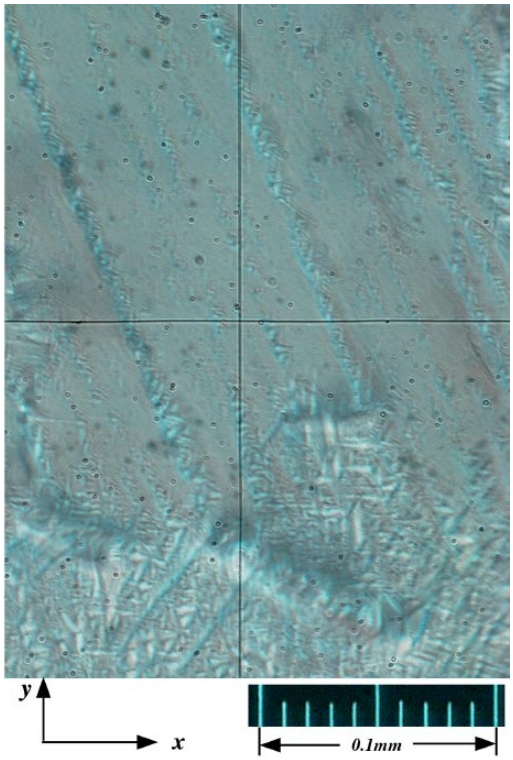

Fig. 1. Distribution of phase boundaries and domain walls during cooling below the phase transition temperature that relates the phases I and II of TMCC. The Cartesian coordinate system used for quantitative angle measurements is sketched.

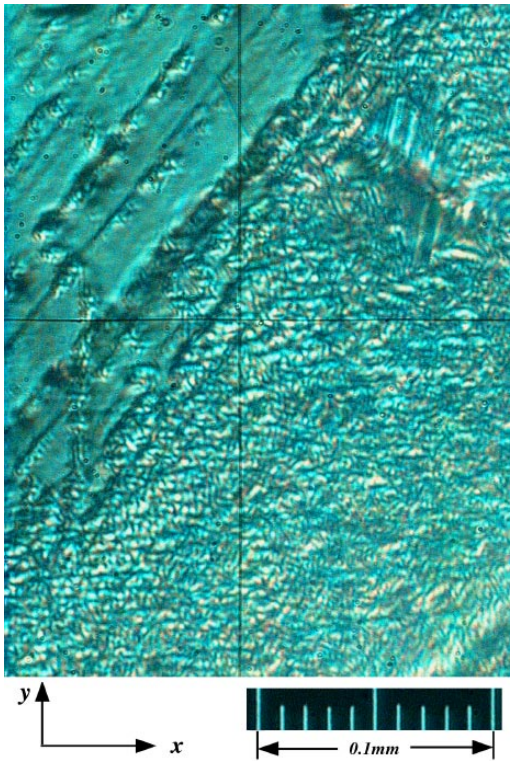

Fig. 2. Distribution of the phase boundaries and domain walls below the I–II phase transition temperature during the heating process.

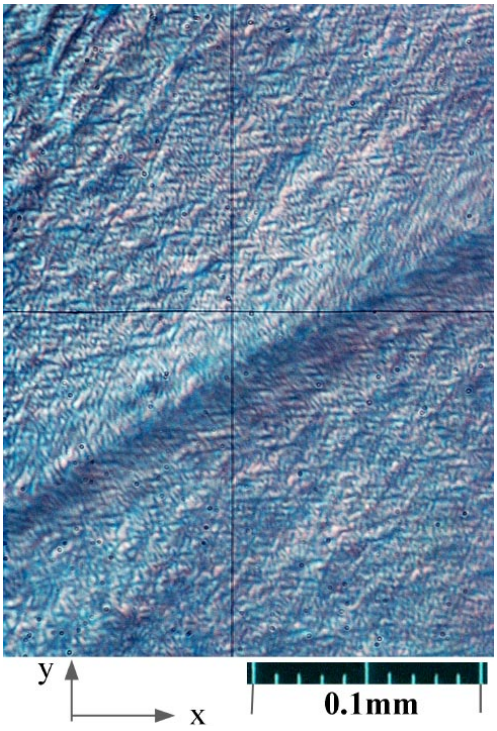

Fig. 3. Domain structure of the ferroelastic phase II of TMCC.

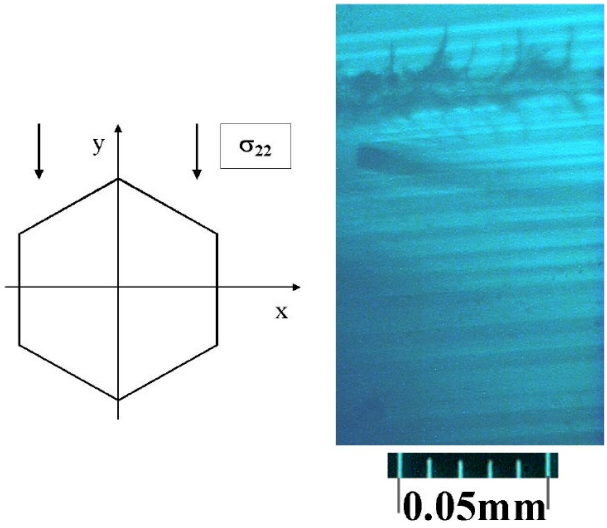

Fig. 4. Domain structure of the ferroelastic phase II after the domain switching provoked by the application of a compressive stress σ_{22}. The relative position of the sample is also represented in the figure.

other ferroelastic crystals. The domain walls, which belong to the same "family" (*i.e.* separating the same pair of orientation states) do not form straight and parallel lines. Again the angles that make the domain walls with the crystallographic axes and between themselves are very difficult to measure given their shape and their very complicated distribution. The value of the angles between the domain walls and the crystallographic axes can not be explained using only the classical symmetry approach of Sapriel [15]. There are also domains belonging to the same orientation state that are rotated relatively one to each other by small angles around an axis (the six-fold axis of the hexagonal phase in the case of TMCC) common to all of them. These observations confirm the results of the X-ray measurements given in reference [7]. The whole diffraction pattern of phases II and III can only be indexed assuming the existence of four identical domains (and eight additional domains obtained by the successive application of the threefold axis of phase I lost during the phase transition to phase II) slightly misoriented.

To confirm the ferroelastic character of the observed domains an external, compressive and unidirectional (along the y-axis) mechanical stress (σ_{22}) was applied to the sample. Figure 4 shows that the domain structure has changed drastically. Domains are now bigger and it is clear that only two types of domains, separated by plane domain walls that make angles of 5° with the x-axis, exist. Also domain walls forming angles of 98.8° are observed. When the stress is switched off new walls at angles of 35.0° appear but the dimensions of the domains do not change. Within the monoclinic phase II there is no change in the position of the domain walls when temperature is varied.

No changes in the distribution and size of domains are observed below the phase transition temperature (T_c = 104.4 K) to the phase III.

4 Discussion

TMCC exhibits a first order ferroelastic phase transition at 118 K. At this temperature the crystal system changes from hexagonal with the space group $P6_3/m$ $Z = 2$ to monoclinic $P2_1/m$ $Z = 2$ (6/mF2/m [14]). Such symmetry change provokes the appearance of a ferroelastic domain structure. According to the usual symmetry considerations the number of different orientation states (domains) for this type of phase transition (determined by the ratio of the point group order of the paraelastic phase to the point group order of the ferroelastic one) should be 3 with 6 permissible domain walls among them [15].

In general, the orientation of any type of ferroelastic domain walls between two adjacent domains S_1 and S_2 is given by

$$[e_S(S_1)_{ij} - e_S(S_2)_{ij}]x_i x_j = 0 \qquad (1)$$

where in the case of TMCC

$$e_S(S_k)_{ij} = e(S_k)_{ij} - \frac{1}{3}\sum_{i=1}^{3} e(S_i)_{ij} \qquad (2)$$

are the components of the spontaneous strain tensor of the k-orientation state being $e(S_k)$ the strain tensor of the k-orientation state in the monoclinic phase. This result is based on the condition that the spontaneous strain

of two adjacent domains must be identical at the domain boundary. Equation (1) splits into a product of two linear equations (representing two planar walls) if the condition

$$\det[e_S(S_1)_{ij} - e_S(S_2)_{ij}] = 0 \tag{3}$$

is satisfied. The strain tensor of the monoclinic group 2/m has the form:

$$e(S_1) = \begin{pmatrix} e_{11} & e_{12} & 0 \\ e_{12} & e_{22} & 0 \\ 0 & 0 & e_{33} \end{pmatrix}. \tag{4}$$

The two remaining orientation states S_2 and S_3 and their corresponding strain tensors $e(S_2)$ and $e(S_3)$ can be generated by the successive application, on S_1 and $e(S_1)$, of 120° and 240° rotations around the hexagonal c-axis. Using equation (2), the spontaneous strain tensors $e_S(S_k)$ for the orientation states S_1, S_2 and S_3 can be calculated:

$$\begin{aligned} e_S(S_1) &= \begin{pmatrix} -A & B & 0 \\ B & A & 0 \\ 0 & 0 & 0 \end{pmatrix} \\ e_S(S_2) &= \begin{pmatrix} \frac{1}{2}(A+\sqrt{3}B) & \frac{1}{2}(\sqrt{3}A-B) & 0 \\ \frac{1}{2}(\sqrt{3}A-B) & -\frac{1}{2}(A+\sqrt{3}B) & 0 \\ 0 & 0 & 0 \end{pmatrix} \\ e_S(S_3) &= \begin{pmatrix} \frac{1}{2}(A-\sqrt{3}B) & -\frac{1}{2}(\sqrt{3}A+B) & 0 \\ -\frac{1}{2}(\sqrt{3}A+B) & -\frac{1}{2}(A-\sqrt{3}B) & 0 \\ 0 & 0 & 0 \end{pmatrix} \end{aligned} \tag{5}$$

where $A = 0.5(e_{22} - e_{11})$, $B = e_{12}$ and e_{11}, e_{22}, e_{12} are the non zero components of the strain tensor in the monoclinic phase. For the 6/mF2/m transition these components are given [16] by:

$$\begin{aligned} e_{11} &= \left(\frac{a\sin\gamma}{a_0 \sin 120°}\right) - 1 \\ e_{22} &= \left(\frac{b}{a_0}\right) - 1 \\ e_{12} &= \frac{1}{2}\left(\frac{a\cos\gamma}{a_0 \sin 120°} - \frac{b\cos 120°}{a_0 \sin 120°}\right) \end{aligned} \tag{6}$$

where a, b, and γ are the relevant cell parameters of the low temperature phase II. a_0 is the cell parameter of an average hexagonal structure extrapolated from the high temperature phase to the temperature where the phase II is known. It was calculated using the condition that for this hypothetical hexagonal structure the mean strain tensor components (the last term in Eq. (2)) vanish.

Using the same arguments as in the case of the domain walls, it can be demonstrated that the phase boundaries between the paraelastic phase and the orientation states S_k appearing during the phase transition are given by the equation [13,17,18]:

$$e_S(S_k)_{ij} x_i x_j = 0. \tag{7}$$

With the cell parameters of the phase II [7], $a = 9.3340$ Å, $b = 8.7963$ Å, $c = 6.6880$ Å and $\gamma = 120.958°$, the values of $a_0 = 9.0194$ Å, $A = -2.47\times10^{-2}$ and $B = -2.58\times10^{-2}$ can be calculated and therefore the equations of the domain walls and the values of the angles their form with the x-axis. The results are given in Table 1. According to the classification given by Sapriel [15], all these domain walls are W-type, *i.e.*, their orientation depends on the actual values of the different components of the spontaneous strain. In Table 2 the equations (Eq. (7)) of the phase boundaries and the approximate (A and B have been calculated at a temperature below the phase transition temperature) tilt angles respect to the x-axis are given.

Comparing the calculated values of the angles (Tabs. 1 and 2) with the measured ones, it can be concluded that during cooling the first orientation state that appears after the phase transition is S_1. The phase boundary between this orientation state and the paraelastic phase forms an angle of 111.6° (Fig. 1) which agrees nicely with the calculated ($\beta_2 = 111.9°$) one. The existence of domain walls inside the strips (see Fig. 1) at approximately 60° and 160° with respect to the x-axis indicates that immediately after the phase transition appear S_2 and S_3. The relatively large difference between the measured and the calculated values is due to the error in measurements (domain walls are slightly bent) and also to the fact that the values used for A and B are not the actual values they possess at the phase transition. Simultaneously in small areas of the sample phase boundaries (at $\beta_4 = 141.9°$) corresponding to the S_2 domain are observed. However during heating the phase boundary (Fig. 2) forms an angle of 50.5° ($\beta_3 = 51.9°$) with the x-axis. It points out that the orientation state S_2 is the last one that transforms into the paraelastic phase. These results suggest that the states S_1 and S_2 hold the extreme values for the phase boundary energy possibly due to stress fields induced by the experimental conditions.

The effect of an external mechanical stress on a twinned crystal can be modelled easily [13,16,19] considering only the part of the thermodynamic potential (the free enthalpy) $F(S_k)$, which describes the interaction energy of each ferroelastic domain with an external mechanical stress in the limits of the linear theory of elasticity. Hence:

$$F(S_k) = -e_S(S_k)_{ij}\sigma_{ij} \tag{8}$$

where σ_{ij} are the tensor components of the mechanical stress. The spontaneous deformation energy for the phase II of TMCC in each orientation state is then expressed as:

$$\begin{aligned} F(S_1) &= A(\sigma_{11} - \sigma_{22}) - 2B\sigma_{12} \\ F(S_2) &= \frac{1}{2}(A+\sqrt{3}B)(\sigma_{22} - \sigma_{11}) - (\sqrt{3}A - B)\sigma_{12} \\ F(S_3) &= \frac{1}{2}(A-\sqrt{3}B)(\sigma_{22} - \sigma_{11}) + (\sqrt{3}A + B)\sigma_{12}. \end{aligned} \tag{9}$$

Table 1. Equations, written in the orthogonal system, of the planar domain walls separating pairs of ferroelastic states (denoted by S_1, S_2 and S_3). The numerical values for s, p and t have been obtained as explained in the text. α_1,..., α_6 are the theoretical tilt angles of the domain walls with respect to the x-axis.

$S_1 - S_2$	$S_1 - S_3$	$S_2 - S_3$
y = - s x y = x/s	y = - p x y = x/p	y = - t x y = x/t
$s = \frac{3B - \sqrt{3}A + 2\sqrt{3(A^2+B^2)}}{3A + \sqrt{3}B}$	$p = \frac{3B + \sqrt{3}A + 2\sqrt{3(A^2+B^2)}}{3A - \sqrt{3}B}$	$t = \frac{1}{B}\left(-A + \sqrt{A^2+B^2}\right)$
s = -0.75	p = 0.12	t = 2.3
$\alpha_1 = 36.9^o$ $\alpha_2 = 126.9^o$	$\alpha_3 = 6.9^o$ $\alpha_4 = 96.9^o$	$\alpha_5 = 66.9^o$ $\alpha_6 = 156.9^o$

Table 2. Equations, written in the orthogonal system, of the phase boundaries between the three ferroelastic states (S_1, S_2 and S_3) and the paraelastic phase. β_1,..., β_6 are the theoretical tilt angles of the phase boundaries with respect to the x-axis.

S_1	S_2	S_3
y = H x	y = K x	y = L x
$H = \frac{1}{A}\left(-B \pm \sqrt{A^2+B^2}\right)$	$K = \frac{(\sqrt{3}A - B) \pm 2\sqrt{(A^2+B^2)}}{A + \sqrt{3}B}$	$L = \frac{-(\sqrt{3}A + B) \pm 2\sqrt{(A^2+B^2)}}{A - \sqrt{3}B}$
$\beta_1 = 21.9^o$ $\beta_2 = 111.9^o$	$\beta_3 = 51.9^o$ $\beta_4 = 141.9^o$	$\beta_5 = 81.9^o$ $\beta_6 = 171.9^o$

Considering the case when only a mechanical stress σ_{22} is applied and using the values of A and B we get:

$$\begin{aligned} F(S_1) &= 2.47 \times 10^{-2}\sigma_{22} \\ F(S_2) &= -3.46 \times 10^{-2}\sigma_{22} \\ F(S_3) &= 1.00 \times 10^{-2}\sigma_{22} \end{aligned} \tag{10}$$

Supposing the stress is compressive ($\sigma_{22} < 0$) we obtain:

$$F(S_1) < F(S_3) < F(S_2) \tag{11}$$

Therefore the switching process occurs in such a way that the domains S_1 and S_3 occupy more and more volume of the crystal at the expense of the S_2 disappearance.

In Figure 4 the consequences of applying a compressive stress σ_{22} are shown. According to the above prediction, only the domain walls between the S_1 and S_3 should be present and forming an angle of 5.0° with the x-axis. This angle is smaller than the calculated one ($\alpha_3 = 1.9°$ in Tab. 1) by 1.9°. Domain walls between S_1 and S_3 at 98.8° were also observed. In this case the measured angle is 1.9° larger than the calculated value ($\alpha_4 = 96.9°$). Therefore in the phase II of TMCC it is clear that the two walls, which according to the classical symmetry approach [15] should be at 90°, form between them an angle of 93.8°. In stress free samples the domain walls between S_1 and S_2 are tilted 35.0°. Again this angle is smaller by 1.9° than that listed in Table 1 ($\alpha_1 = 36.9°$).

The possibility of small angular misorientations of coherent domain walls around an axis common to all of them (in this case the c-axis) was also explained by Sapriel [15], although a quantitative method for calculating the rotation angle φ was given later by Shuvalov and Dudnik [12,13]. The possible values for φ are related to the absolute value of the eigenvalues of $e_S(S_1) - e_S(S_2)$. In the case of TMCC the predicted values should be equal to or a multiple of $\varphi = \sqrt{3(A^2 + B^2)}$ whose theoretical value (3.55°) is in very good agreement with the one (3.8°) obtained here by direct microscopic measurements and also with the results (3.6(2)°) of X-ray measurements [7].

One of the authors (IP) is particularly indebted to the Basque Government for financial support. This work has been supported by the University of the Basque Country and the Basque Government through the following projects: UPV project 060.310-616/98, UPV project EB098/97 and GV project PI 97/71.

References

1. K. Gesi, Ferroelectrics **137**, 209 (1992).
2. M.N. Braud, M. Couzi, N.B. Chanh, C. Courseille, B. Gallois, C. Hauw, A. Meresse, J. Phys. Cond. Matt. **2**, 8209 (1990).
3. S. Mulla-Osman, D. Michel, Z. Czapla, W.D. Hoffmann, J. Phys. Cond. Matt. **10**, 2465 (1998).
4. P.S. Peercy, B. Morosin, G.A. Samara, Phys. Rev. B **8**, 3378 (1973).
5. M. Couzi, Y. Mlik, J. Raman Spectrosc. **17**, 117 (1986).
6. J. Díaz Hernández, G. Aguirre-Zamalloa, I. Ruiz-Larrea, A. Lopez-Echarri, T. Breczewski, M.J. Tello, J. Phys. Cond. Matt. **9**, 3399 (1997).
7. I. Peral, G. Madariaga, A. Pérez-Etxebarria, T. Breczewski, Acta Cryst. B **56**, 215 (2000).
8. G. Aguirre-Zamalloa, G. Madariaga, M. Couzi, T. Breczewski, Acta Cryst. B **49**, 691 (1993).
9. D. Visser, G.J. McIntyre, Physica B **156/157**, 259 (1989).
10. S. Teraoka, T. Kambe, N. Koido, S. Hirai, K. Nagata, J. Magn. Magn. Mater. **140-144**, 1659 (1995).
11. W. Knop, M. Steiner, Solid State Commun. **51**, 521 (1984).
12. L.A. Shuvalov, E.F. Dudnik, S.V. Wagin, Ferroelectrics **65**, 143 (1985).
13. E.F. Dudnik, L.A. Shuvalov, Ferroelectrics **98**, 207 (1989).
14. K. Aizu, J. Phys. Soc. Jpn **28**, 706 (1970).
15. J. Sapriel, Phys. Rev. B **12**, 5128 (1975).
16. E.K.H. Salje, *Phase Transitions in ferroelastic and co-elastic crystals* (Cambridge University Press, 1990).
17. C. Boulesteix, B. Yangui, M. Ben Salem, C. Manolikas, S. Amelinckx, J. Phys. France **47**, 461 (1986).
18. J. Dec, Phase Transitions **45**, 35 (1993).
19. V.K. Wadhawan, Phase Transitions **3**, 3 (1982).